

EL NIÑO IMPACT ON POLAR MOTION PREDICTION ERRORS

W. Kosek

Space Research Centre, Polish Academy of Sciences, Warsaw, Poland
kosek@cbk.waw.pl

D.D. McCarthy, B.J. Luzum

U.S. Naval Observatory, Washington D.C., USA
dmc@maia.usno.navy.mil , bjl@maia.usno.navy.mil

Abstract. The polar motion prediction is computed as a least-squares extrapolation of the polar motion data. The least-squares model consists of a Chandler circle with constant or variable amplitude, annual and semiannual ellipses, and a bias. The model with constant amplitude of the Chandler oscillation is fit to the last three years of polar motion data and the model with variable amplitude of the Chandler oscillation is fit to the whole time series ranging from 1973.0 to 2001.1. The variable amplitude of the Chandler oscillation is modeled from the envelope of the Chandler oscillation filtered by the Fourier transform band pass filter from the long-term IERS EOPC01 polar motion series. The accuracy of the polar motion prediction depends mostly on the phase variation of the annual oscillation, which is treated as a constant in the least-squares adjustment. There were two significant changes of the annual oscillation phase of the order of 30° before the two El Niño events in 1982/83 and 1997/98.

1. Introduction

The accuracy of the combined pole coordinate data determined from the SLR, VLBI, GPS and DORIS space techniques is of the order of 0.2 milliseconds of arc (mas). Such precise polar motion data cannot be predicted with the accuracy corresponding to their observational accuracy. Usually, the prediction error for a few days in the future is several times greater than the pole coordinate data determination error. Such limited prediction accuracy is caused by irregular amplitudes and phases of the semiannual (Kosek and Kołaczek 1997) and shorter period oscillations (Eubanks et al. 1988; Kosek et al. 1995a,b). Subseasonal variations of polar motion with periods shorter than half a year have variable and nonstationary phases and amplitudes (Kosek 1995; Popiński and Kosek 1995; Schuh and Schmitz-Hübsch 2000), thus their prediction cause some problems (Kosek 1997, 2000; Kosek et. al. 1998). The forward and backward autocovariance and autoregressive predictions applied to short-period polar motion data reveal the biggest irregular variations in 1980-81, 1984-85, 1988, 1995 (Kosek 2000).

Accuracy of polar motion prediction depends on the variable Chandler oscillation amplitude (Yatskiv et al. 1972; Nastula et al. 1993; Damljanović et al. 1997; Vondrak 1985, 1989; Kołaczek and Kosek 1998; Schuh et al. 2001b) and period/phase (Okubo, 1982; Lenhardt and Groten 1987; Vicente and Wilson 1997; Gilbert et al. 1998). The Chandler oscillation amplitude varies with periods of 75, 40, 30 and 20 years (Kołaczek and Kosek 1998). Periodic variations between 40 and 50 years of the Chandler wobble and 5-6, 8-9, and 18-20 years of the annual wobble parameters were found using wavelet analyses techniques (Schuh et al. 2001a). Poor accuracy of polar motion prediction can be caused by a variable phase or period

of the annual oscillation (Kosek et al. 2000; Schuh et al. 2001a). Poor accuracy of long term polar motion prediction can be caused by mismodelling of linear drift and decadal variations of polar motion (Lambeck 1980; Johmann 1993; McCarthy and Luzum 1996; Vondrak 1999b). Analysis of long term polar motion series obtained from re-analysis of optical astrometry using HIPPARCOS catalogue Vondrak (1999a) shows that the linear drift of polar motion during the last century was of the order of 3.31 ± 0.05 mas/year in the direction of $76.1 \pm 0.80^\circ$ (Schuh et al. 2001a). Standard Fourier and Wavelet analyses of these data show prograde and retrograde decadal variations in these polar motion time series ranging from 7 to 86 years from which the dominant retrograde 30-year Markowitz (1970) wobble is stable and all the oscillations with periods shorter than 20 years are irregular (Schuh et al. 2001a).

In some of the prediction methods of Earth orientation parameters (EOP - polar motion and LOD, or UT1-UTC) the parameters of harmonic functions including bias and drift were estimated and extrapolated into the future (Zhu 1981, 1982; Chao 1984; McCarthy and Luzum 1991b; McCarthy and Luzum 1996; Malkin and Skurikhina 1996). To predict LOD or UT1-UTC the stochastic tools, e.g. Kalman filter (Freedman et al. 1994) or ARMA (Auto-Regressive Moving Average) (Hamdan and Sung 1996) were used. It has been found that Atmospheric Angular Momentum (AAM) and its forecast data are helpful in generating accurate near-real-time estimates of UT1 and LOD and in improving short-term predictions of these quantities out to about 10 days (Freedman et al. 1994). The EOP were recently predicted using artificial neural networks and the comparison of their results with results of other prediction methods proves that they are very appropriate tools to predict the EOP (Schuh et al. 2001b). Polar motion was recently predicted with an accuracy similar to other methods by the autocovariance prediction method applied to the pole coordinate data transformed into polar motion radius and angular distance (Kosek 2001).

The current prediction method of polar motion data carried out in the IERS (International Earth Rotation Service) Rapid Service/Prediction Center is the least-squares extrapolation of a Chandler circle, annual and semiannual ellipses and a bias fit to the last 3 years of combined pole coordinate data (McCarthy and Luzum 1991b). This least-squares extrapolation, together with the autocovariance prediction of the polar motion extrapolation residuals, enables prediction of polar motion for about 50-250 days in the future with approximately twice the accuracy of the least-squares prediction model (Kosek et al. 1998). However, it was noticed that predictions were less accurate before the last 1997/98 El Niño event due to the decrease of the annual oscillation period (Kosek et al. 2000).

2. Data

The IERS EOPC01 in the years 1846.0 to 2000.0 (IERS 2001) and the NEOS pole coordinates data in the years 1973.0 to 2001.1 (USNO 2001) were used in the analysis. The sampling interval of the IERSC01 pole coordinates is 0.10 and 0.05 year before and after 1880, respectively, and the sampling interval of the NEOS pole coordinates data is equal to 1 day. To make the whole IERSC01 pole coordinates data equidistant, they were interpolated using 0.05-year sampling intervals before 1880. The NEOS series is based on a weighted cubic spline. The observational input are corrected for possible bias and rate with respect to the IERS C04 series. The weights used in the combination are proportional to the inverse square of the estimated accuracy of input data (McCarthy and Luzum 1991a).

Monthly sea surface temperature anomalies Niño 1+2 (0-10S)(90W-80W), Niño 3 (5N-5S)(150W-90W), Niño 4 (5N-5S) (160E-150W), Niño 3.4 (5N-5S)(170-120W) in the years 1950 to 2001.0 from the Climate Prediction Center were used in the analysis (NOAA 2001).

3. Amplitude and phase variations of the Chandler and annual oscillations of polar motion

The envelopes of the Chandler and annual oscillations can be computed if they are filtered properly by a band pass filter from the polar motion time series. The accuracy of a filtered oscillation by any band pass filter at the end and at the beginning of time series is affected by filtering errors, so some prolongation into the future of the polar motion data is necessary to cut off the ends after filtering.

To compute such filtered oscillations, the IERS EOPC01 extended by the NEOS pole coordinate data and their prediction to 2002.4 were used. The NEOS pole coordinate data were predicted using the least-squares extrapolation of the Chandler circle, annual and semiannual ellipses and a bias fit to the last 3 years of data, and then these data together with their prediction were interpolated at 0.05-yr sampling intervals. To filter the Chandler and annual oscillations using a band pass filter, their mean periods must be known. These periods were computed from the IERS EOPC01 pole coordinates data in the years 1900.0 to 2000.0 using the MESA (Burg 1967) with an optimum filter length estimated from the Rovelli-Vulpiani criterion (Rovelli and Vulpiani 1983) and by the Fourier transform band pass filter (FTBPF) spectral analysis with parabolic transfer function ($\lambda = 0.002$) (Popiński and Kosek 1995, Kosek 1995) (Table 1). Additionally, the FTBPF spectral analysis enables computation of the mean amplitudes of oscillations as the square root of the FTBPF spectrum multiplied by $\sqrt{2}$ in the case of real-valued time series and the mean radii of prograde (positive periods) and retrograde (negative periods) oscillations in the case of complex-valued time series (Kosek 1995).

Table 1. The periods and amplitudes of the Chandler and annual oscillations computed by the MESA and the FTBPF spectral analysis from the IERS EOPC01 pole coordinates from 1900.0 to 2000.0.

Pole coordinates data		x		y		x - iy		
MESA	Periods (years)	1.183	1.002	1.184	1.001			
FTBPF	Periods (years)	1.185	1.001	1.185	1.001	1.182	0.999	-1.000
	Amplitude/radius* (arcsec)	0.1076	0.0621	0.1076	0.0530	0.1521*	0.0813*	0.0074*

The Chandler and annual oscillations with central periods of 1.182yr and 1.000yr, respectively, were filtered from the extended IERS EOPC01 pole coordinate data by the FTBPF using optimum frequency bandwidth. The optimum frequency bandwidth $\lambda = 0.007$ was chosen so that the variance of the residuals after subtracting the filtered Chandler and annual oscillations was a minimum. The EOPC01 polar motion residuals after subtracting such filtered Chandler and annual oscillations are shown in Figure 1.

In the case of the Chandler and annual oscillations with similar periods, their resolution improves when the time span of polar motion data becomes longer. To check whether the Chandler and annual oscillations were separated well by the FTBPF, the running correlation coefficients between their envelopes were computed. The running correlation coefficients values between the envelopes of the filtered Chandler and annual oscillations in x and y pole

coordinate data, captured by the boxcar window with a length of 30 years, are shown in Figure 2. Notice that for the variable amplitude Chandler oscillation, the correlation coefficient values between the envelopes in x and y are close to 1. In the case of the envelopes of the annual oscillation in x and y, such correlation coefficients increase during the last 100 years from 0.6 to 0.9. The running correlation coefficient values between the envelopes of the filtered Chandler and annual oscillations varies from -0.4 to 0.4 and after 1970 begin to decrease to the level of -0.7 and -0.4 for x and y, respectively. This means that the computed envelopes of the Chandler and annual oscillations are not independent. Possible reasons for the large correlation coefficient in x (-0.7) in the 1980s could be poor separation of the Chandler and annual oscillations by the FTBPF or some common geophysical cause of excitation of the Chandler and annual oscillation amplitudes.

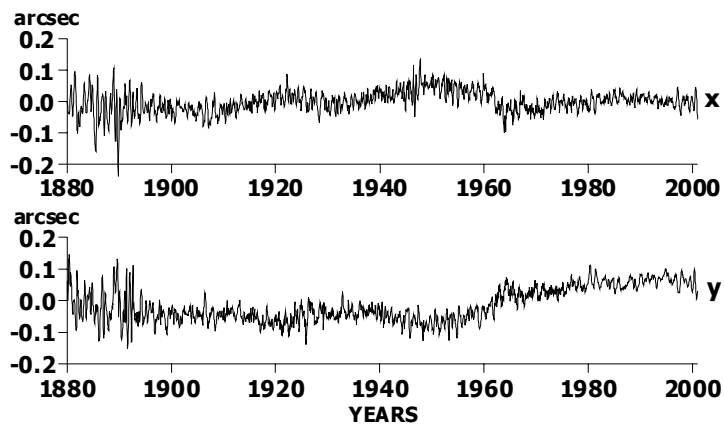


Fig. 1. The x, y IERS EOPC01 polar motion residuals after subtracting the Chandler and annual oscillations filtered by the FTBPF ($\lambda=0.007$).

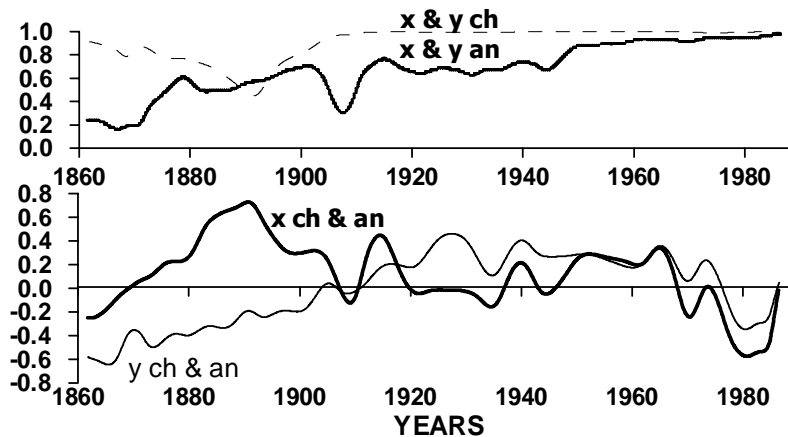


Fig. 2. The running correlation coefficient values captured by the running boxcar window with the length of 30 years between the envelopes of the Chandler (dashed line) and annual (heavy line) oscillations in x (thick line) and y (thin line) pole coordinate data.

To compute the models of the Chandler and annual oscillation envelopes, the periods of oscillations in the envelope time series ranging from 1880 to 2000 were computed by the MESA with optimum filter length computed by the Rovelli-Vulpiani (1983) criterion (Table 2). Similar periods of 75, 40, 30 and 20 years in the envelopes of the Chandler oscillations have been previously found by Kołaczek and Kosek (1998). Introduction of the amplitude

variations models of the Chandler and annual oscillations into the least-squares adjustment could decrease the polar motion prediction errors.

Table 2. Periods of the most energetic oscillations in the envelopes of the Chandler and annual terms in x and y IERS EOPC01 pole coordinates data found by the MESA with the Rovelli-Vulpiani criterion.

Envelope of	Periods in years				
X Chandler	73	36.8	20.3	13.9	10.4
Y Chandler	70	37.6	19.3	13.4	10.0
X Annual	57	23.5	16.3	10.5	
Y Annual	45	25.8	15.4	11.2	

To compute the models of the envelope of the Chandler oscillation for the five chosen mean periods of 70, 37, 19.8, 13.6 and 10.2 years (Table 2), the amplitudes and phases were computed by the least-squares method using different lengths of the envelope data. Before the least-squares method was applied, the secular variations were subtracted using a robust straight-line estimate (Priestley 1981). The amplitudes and phases of the best fit least-squares models of the Chandler oscillation amplitude computed from the last 50 years of data for x and y pole coordinates are given in Table 3. Notice that the most energetic oscillations in the envelopes of the Chandler oscillations are oscillations with periods of about 70 and 40 years.

Table 3. Periods, amplitudes and phases of the envelope models of the Chandler oscillation amplitude computed by the least-squares method from 1950 to 2000. The RMS are equal to 3.0 and 4.4 mas in x and y, respectively.

	Periods (years)	70	37	19.8	13.6	10.2
X	Amplitude (mas)	32.4	48.7	9.4	11.3	6.5
	Phase (radians)	1.55708	1.47134	0.31552	5.99178	5.85967
Y	Amplitude (mas)	28.8	55.0	14.0	12.8	7.4
	Phase (radians)	1.10620	1.41719	0.35901	5.96999	5.83038

Robust straight line $z=a(t-1950)+b$: in x $a=-8.354592E-05$, $b=0.1764$, in y $a=-8.245441E-06$, $b=0.1735$.

To compute the models of the annual oscillation envelope for four chosen periods of 50, 24, 15.8 and 10.8 years (Table 2), the amplitudes and phases were computed by the least-squares method together with the robust straight line estimates for the x and y envelope data from 1960 to 2000 (Table 4). The amplitudes in the envelopes of the annual oscillation in x and y are also variable. However, their changes are much smaller than for the Chandler oscillation. Thus, there is no need to introduce information about the model of the annual oscillation envelope into the polar motion prediction program.

In order to check whether the amplitude variations of the Chandler and annual oscillations computed by the FTBPF were estimated well, they were also computed by the least-squares model of a Chandler circle, annual and semiannual ellipses and a bias fit to the three-year NEOS pole coordinate data sliding with a step of 7 days along the whole data interval from 1973.0 to 2001.1. The least-squares amplitudes of the Chandler and annual oscillations captured by the running three-year boxcar window are shown together with the corresponding envelopes of the filtered Chandler and annual oscillations in Figure 3a. Notice that the envelopes of the oscillations filtered by the FTBPF Chandler and annual are in a good agreement with their corresponding least-squares amplitudes. Some disagreement of these least-squares amplitudes with the corresponding envelopes at the end of the series could be

caused by the increase of the FTBPF filtering errors there. Since the Chandler oscillation envelope model is introduced to the least-squares adjustment of the entire pole coordinate data, it may slightly affect the polar motion prediction errors at lower frequencies due to mismodelling of the Chandler amplitude change.

Table 4. Periods, amplitudes and phases of the envelope models of the annual oscillation amplitude computed by the least-squares method in 1960-2000. The RMS are equal to 4.2 and 3.5 mas in x and y, respectively.

	Periods (years)	50	24.6	15.8	10.8
X	Amplitude (mas)	8.5	2.6	3.6	8.5
	Phase (radians)	5.62201	3.34974	2.48970	5.40311
Y	Amplitude (mas)	3.1	3.1	4.4	6.0
	Phase (radians)	5.50385	3.30756	3.30756	5.35589

Robust straight line $z=a(t-1950)+b$: in x $a=-4.259076E-04$, $b=1.74199$, in y $a=-9.064993E-04$, $b=1.8767$.

The least-squares phases of the Chandler and annual oscillations captured by the running three-year boxcar windows are shown in Figure 3b. Notice that the phase variations of the annual oscillation in x and y pole coordinate data are of the same order and the difference between the maximum and minimum phase is of the order of 50° during the last 20 years. After 1982 the phase variations of the Chandler oscillation, which are of the order of 10° , are less than the phase variations of the annual oscillation (Fig. 3b). Before 1982 a big increase of the phase of the Chandler oscillation of the order of 40° during 5 years can be noticed (Fig. 3b). Wavelet analysis of the Chandler wobble identified 3 large phase jumps with different durations in 1913, 1926 and 1980 during the time period 1890-1997 (Gilbert et al. 1998).

There are significant increases of the annual oscillation phase of the order of $30^\circ-40^\circ$ before the El Niño events in 1982/83 and 1997/98. Notice that the decrease of the phase values of the annual oscillation correspond to the maxima of El Niño events in 1982/83 and in 1997/98, so El Niño data seem to be mostly correlated with the annual oscillation phase changes.

To check the relations between El Niño and the annual oscillation parameters, the correlation coefficients between the Niño 1+2, Niño 3, Niño 4, Niño 3.4 data and amplitude/phase variations of the annual oscillations were computed in the two time periods 1980-2000 and 1990-2000 (Table 5).

Table 5. The correlation coefficient values between the Niño 1+2, Niño 3, Niño 4, Niño 3.4 data and the amplitudes/phase changes of the annual oscillation. * denotes correlation coefficients values significant at 90% confidence level.

Time period	1980 - 2000				1990 - 2000			
	LS amplitude		LS phase change		LS amplitude		LS phase change	
degrees of freedom	n=26		n=36		n=13		n=18	
coordinate	x	y	x	y	x	y	x	y
Niño 1+2	0.273*	0.275*	-0.195	-0.177	0.422*	0.439*	-0.346*	-0.318*
Niño 3	0.206	0.205	-0.161	-0.145	0.253	0.277	-0.329*	-0.302
Niño 4	-0.084	-0.083	-0.088	-0.058	-0.204	-0.164	-0.232	-0.184
Niño 3.4	0.103	0.104	-0.141	-0.131	0.054	0.086	-0.305	-0.278

The confidence levels for correlation coefficient values were estimated by the Students t-test assuming that the degrees of freedom were estimated as the ratio of data time span and the characteristic correlation time (Rovelli and Vulpiani 1983). The characteristic correlation time is defined in this paper as the time for which the biased autocorrelation estimation of the first difference of the annual oscillation least-squares amplitude or phase time series (Fig. 3a,b) decreases to a small value equal to 0.1. Since the Niño data are treated as independent, the degrees of freedom estimated from them would be greater than those computed from the characteristic correlation time, so the latter would overestimate the confidence levels of correlation coefficient values.

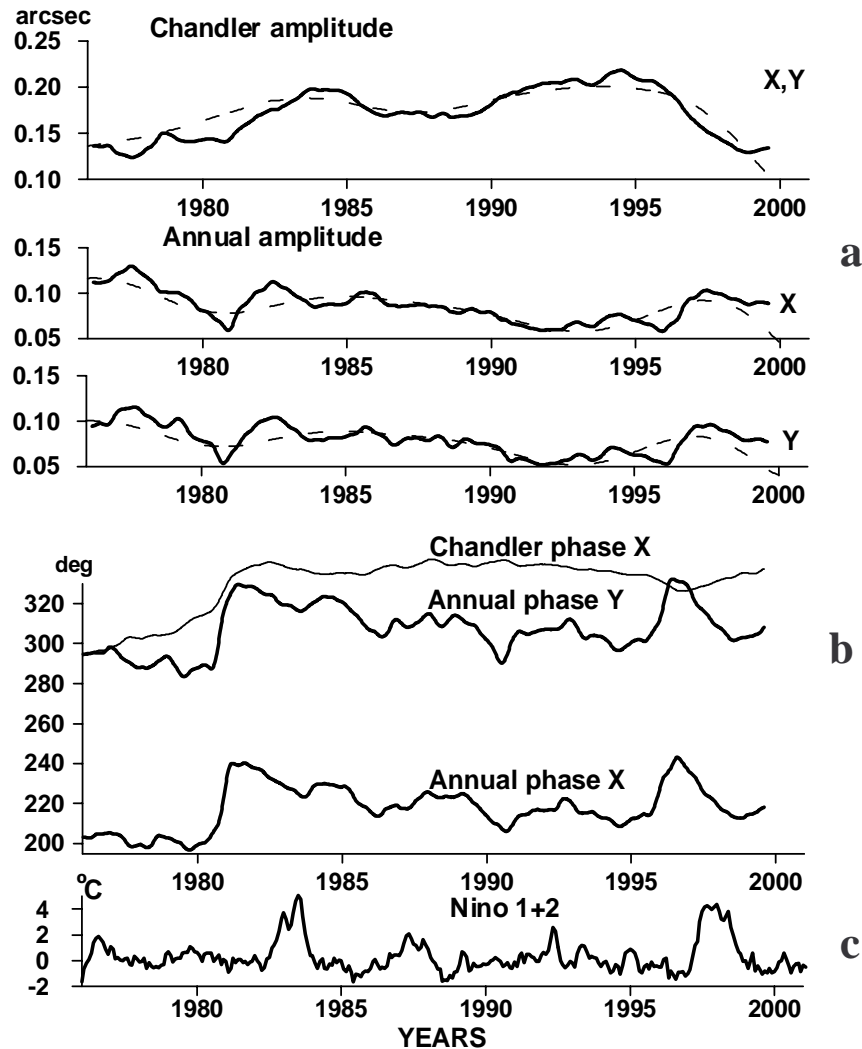


Fig. 3. The envelopes of the Chandler and annual oscillation filtered by the FTBPF (dashed lines) in x and y pole coordinate data a). The least-squares amplitudes a) and phases referred to the epoch 1976.060 (MJD=42800) b) of the Chandler and annual oscillations computed in the three-year running boxcar windows. The Niño 1+2 data c).

Notice that the absolute values of the correlation coefficients are significant at the 90% confidence level for the Niño 1+2 and for the Niño 3 data in the case of the least-squares phase change from 1990 to 2000 (Table 5). The correlation coefficient values between annual oscillation parameters and the Niño 4 or Niño 3.4 data are not significant. The correlation

coefficient values between all Niño data and the phase changes of the annual oscillation computed from the data time span of 1980 – 2000 are not significant either.

4. Polar motion extrapolation residuals

The three-year least-squares extrapolation residuals of pole coordinate data were computed from the three-year NEOS polar motion data after subtracting the least-squares model data consisting of a Chandler circle, annual and semiannual ellipses and a bias. These residuals were shifted by 7 days with respect to each other and their first differences were centered and connected using a trapezoid function (Kosek et al. 1998). The connected three-year extrapolation residuals (Fig. 4) were computed after integrating once the connected differences. Notice that energetic oscillations of y extrapolation three-year residuals usually have longer periods than x extrapolation residuals. The whole least-squares polar motion extrapolation residuals of pole coordinate data (Fig. 5) were computed after subtracting the model of the Chandler circle with variable amplitude (Table 3), annual and semiannual ellipses and a bias from the NEOS polar motion data ranging from 1973.0 to 2001.1.

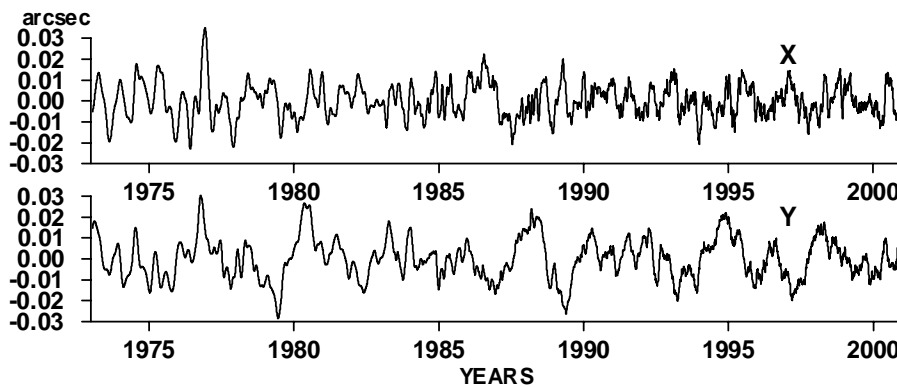


Fig. 4. The connected three-year least-squares polar motion extrapolation residuals of x and y pole coordinate data.

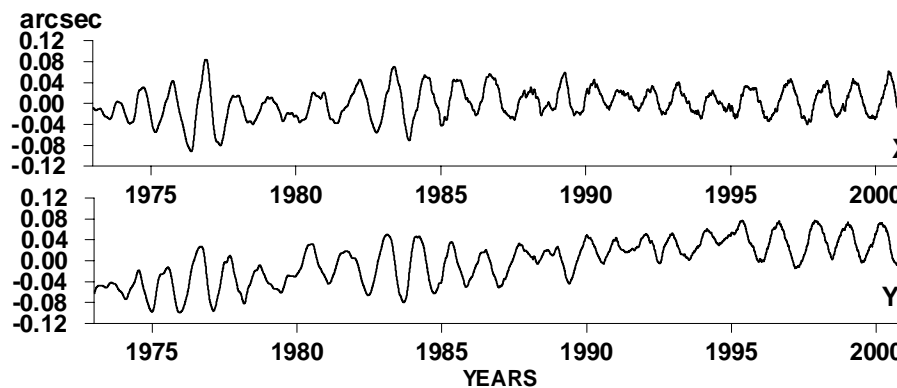


Fig. 5. The entire least-squares polar motion extrapolation residuals of x and y pole coordinate data.

The information about amplitude variations of the Chandler oscillation in the form of the envelope model computed from the envelopes of the filtered Chandler oscillation (Table 3) has been added to the observational equations in the least-square adjustment. The difference between the three-year and the entire least-squares polar motion extrapolation residuals is caused mainly by phase variations of the annual oscillation (Fig. 3b) and possible mismodelling of amplitude variations of the Chandler oscillation (Fig. 3a). Since the phase

variations of the annual oscillation have bigger amplitudes than the phase variations of the Chandler oscillation (Fig. 3b) and variations of the annual oscillation amplitude are negligible, the big amplitudes of the entire polar motion extrapolation residuals (Fig. 5) are mainly caused by the phase variations of the annual oscillation.

To detect the most energetic oscillations in the connected three-year least squares extrapolation residuals, the time-variable Fourier transform band pass filter (FTBPF) spectral analysis was applied (Kosek 1995). The time variable FTBPF amplitude spectrum with the parabolic transfer function ($\lambda=0.0005$) is shown in Figure 6. Notice that the residual amplitudes of the annual and semiannual prograde oscillations do not exceed 2 mas. However, in the case of the Chandler oscillation its residual prograde amplitude can reach the 4-5 mas level. The three-year polar motion extrapolation residuals also contain prograde oscillations with periods of about 0.6-0.7 years which is sometimes called the semi-Chandler wobble (Höpfner 1995; Kosek and Kořaczek 1997; Kosek and Popiński 2000) and from 1.3 to 2.2 years with the amplitudes reaching the 4-5 mas level. The oscillation with a period from 1.3 to 2.2 years has the greatest amplitudes just before the time of the El Niño event in 1982/83 and during the El Niño event in 1997/98. The amplitudes of the retrograde oscillations with periods less than 1 year in the three-year polar motion extrapolation residuals do not exceed 1 mas after 1980.

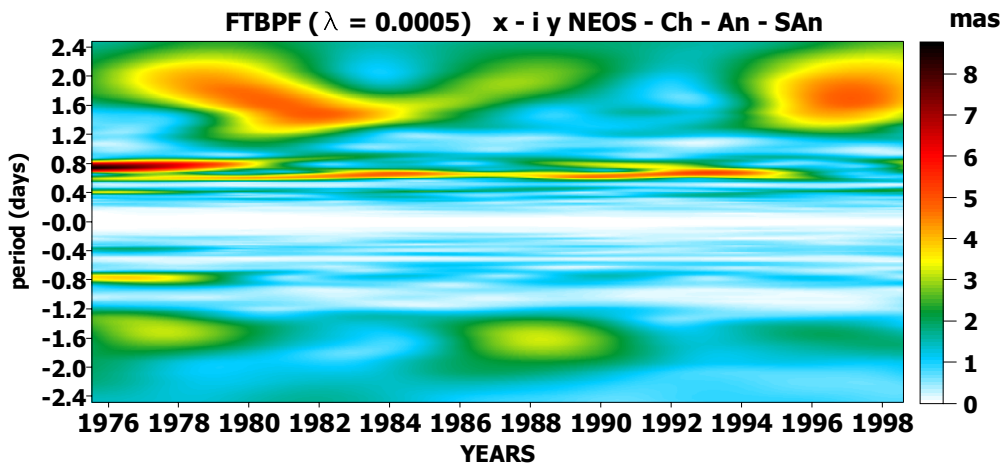


Fig. 6. The FTBPF amplitude spectrum of the connected three-year least-squares polar motion extrapolation residuals of x and y pole coordinate data.

5. Polar motion prediction errors

The absolute values of the difference between the three-year least-squares polar motion extrapolation models and polar motion data from 1 to 50 days in the future are shown in Figure 7. The irregular variations in short-period polar motion prevent high accuracy polar motion prediction. The biggest errors of polar motion prediction of the order of 20 to 30 mas for 30 to 50 days in the future occurred just before or during the two biggest El Niño events in 1982/83 and 1997/98. Big polar motion prediction errors before the 1980s were caused by less accurate polar motion data at that time. Prediction errors in y seem to have a better

correlation with Niño 1+2 data especially during less energetic El Niño events in 1987/88, 1992/93 and 1994/95.

The mean errors of polar motion prediction for 20, 50 and 80 days in the future were computed as the angular distance between the predicted and actual pole positions. To estimate the relationship between El Niño and the polar motion prediction error, the correlation coefficients between the Niño 1+2, Niño 3, Niño 4, Niño 3.4 data and mean polar motion prediction error for 20, 50 and 80 days in the future were computed (Table 6). The confidence levels for correlation coefficient values were estimated by the Students t-test assuming that the degrees of freedom were estimated as the ratio of data time span and the characteristic correlation time. The characteristic correlation time is the time for which the biased autocorrelation estimation of the polar motion prediction error time series (Fig. 7b) decrease to 0.1.

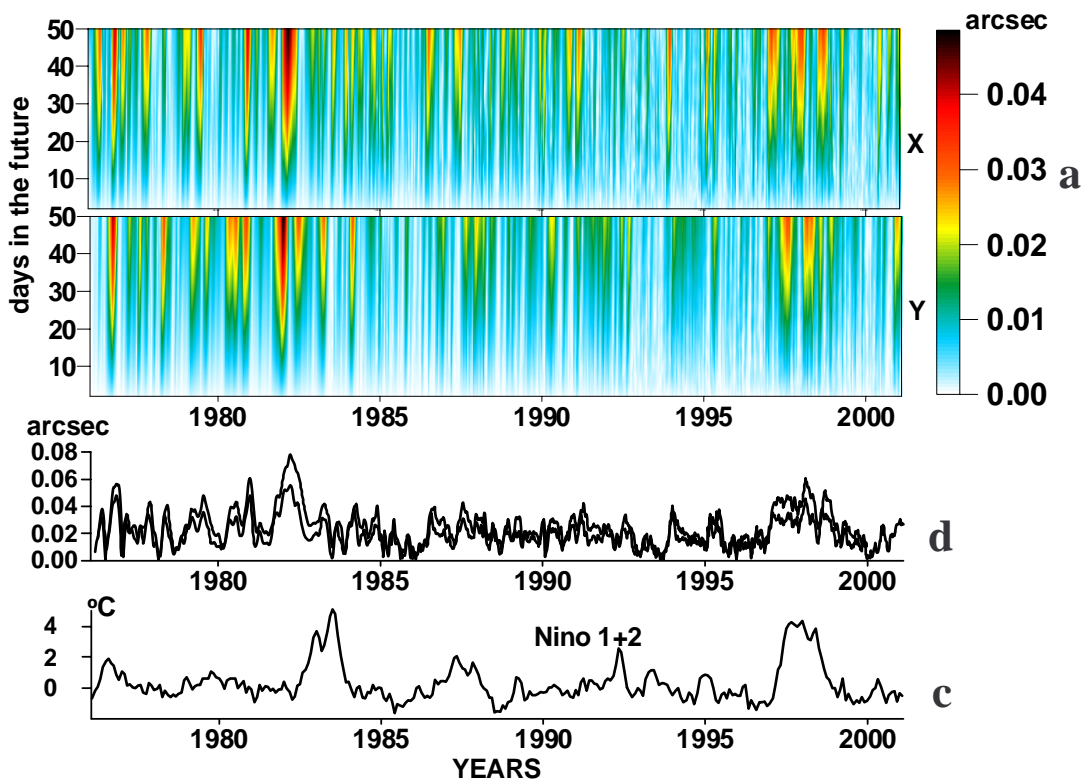


Fig. 7. The absolute values of the difference between x and y NEOS pole coordinate data and their least-squares prediction computed at different starting prediction epochs **a)**, the mean error of polar motion prediction in 50 (lower line) and 80 (upper line) days in the future **b)** and the Niño 1+2 data **c)**.

Notice that the absolute values of the correlation coefficients are significant at the 90% confidence level for the Niño 1+2 and the Niño 3 data for polar motion prediction error 80 days in the future (Table 6). The correlation coefficient values between polar motion prediction errors and Niño 4 or Niño 3.4 data are not significant. The correlation coefficient values between all Niño data and polar motion prediction errors 20 days in the future are not significant either.

Table 6. The correlation coefficient values between the Niño 1+2, Niño 3, Niño 4, Niño 3.4 data and the mean polar motion prediction error in 20, 50 and 80 days in the future. * denotes correlation coefficients values significant at the 90% confidence level.

Days in the future	20		50		80	
Time period	1980-2000	1990-2000	1980-2000	1990-2000	1980-2000	1990-2000
degrees of freedom	n=30	n=15	n=26	n=13	n=24	n=12
Niño 1+2	0.114	0.338	0.345*	0.425*	0.248	0.457*
Niño 3	0.167	0.296	0.252	0.358	0.306*	0.363
Niño 4	0.084	0.090	0.125	0.090	0.155	0.045
Niño 3.4	0.121	0.183	0.206	0.244	0.258	0.237

Conclusions

The cause of the poor accuracy of polar motion predictions can be variable phase or period of the annual oscillation. The Chandler oscillation phase or period is more stable than the annual one. There were two significant increases of the annual oscillation phase of the order of 30°-40° (or decrease of the annual oscillation period by about 30-40 days) before the two biggest 1992/93 and 1997/98 El Niño events.

Correlation coefficients, significant at the 90% confidence level, are found between the Niño data and both the annual oscillation and the polar motion prediction errors. In particular, the correlations between the 50- and 80-day predictions are correlated significantly with the Niño 1+2 and Niño 3 data.

Acknowledgment. This paper was supported by the Polish Committee of Scientific Research project No 8 T12E 005 20 under the leadership of dr. W. Kosek.

References

- Burg J. P. 1967. Maximum Entropy Spectral Analysis, 37th Ann. Int. Meet. Society of Exploration Geophysicists, Oklahoma City, October 31, 1967.
- Chao B. F. 1984. Predictability of the Earth's polar motion, *Bull. Géod.* **59**, 81-93
- Damljanović G., Pejović N. and Djurović D., 1997. The Chandler Nutation for the Period 1949-1985, *Bull. Astron. Belgrade* No **156**, 71-78.
- Eubanks T. M., Steppe J.A., Dickey J.O., Rosen R.D., and Salstein D.A., 1988. Causes of Rapid Motions of the Earth's Pole, *Nature* **334**, No 6178.
- Freedman A. P., Steppe J. A., Dickey J. O., Eubanks T. M., and Sung L.Y., 1994. The short-term prediction of universal time and length of day using atmospheric angular momentum, *Journal of Geophysical Research*, Vol. **99**, No. B4, 6981-6996.
- Gilbert D., Holschneider M., Le Mouél J.-L., 1998. Wavelet Analysis of the Chandler Wobble, *Journ. Geophys. Res.*, Vol. **103**, No B11, 27069-27089.
- Hamdan K. and Sung LY, 1996. Stochastic modelling of length of day and universal time, *Journal of Geodesy*, **70**, 307-320.

- Höpfner J. 1995. Periodische Anteile in der Erdrotation und dem atmosphärischen Drehimpuls und ihre Genauigkeiten, *Zeitschrift für Vermessungswesen*, Heft 1, **120**, Jahrgang, 8-16.
- IERS, 2001. eopc01.dat: Normal values of EOP at 0.05 year intervals covering the period 1846-2000, <http://hpiers.obspm.fr/eop-pc/>
- Johmann H., 1993. Earth rotation and global change. *Adv. Space Res.*, **13(11)**, (11)271-(11)280.
- Kořaczek B. and Kosek W. 1998. Variations of the amplitude of the Chandler Wobble, *Proc. Journées 1998 Systèmes de Référence Spatio-Temporels*, Conceptual, conventional and practical studies related to Earth rotation, Sep. 21-23, Observatoire de Paris, France, 215-220.
- Kosek W. 1995. Time Variable Band Pass Filter Spectra of Real and Complex-Valued Polar Motion Series, *Artificial Satellites, Planetary Geodesy*, No **24**, Vol. 30, No 1, 27-43.
- Kosek W. and Kořaczek B., 1995a. Irregular Short Period Variations of Polar Motion, *Proc. Journées 1995 "Systèmes de Référence Spatio-Temporels"*, Warsaw, Poland, Sep. 18-20, 1995. 117-120.
- Kosek W., Nastula J., and Kořaczek B. 1995b. Variability of Polar Motion Oscillations with Periods from 20 to 150 Days in 1979-1991, *Bull. Géod.*, **69**, 308-319.
- Kosek W., 1997. Autocovariance Prediction of Short Period Earth Rotation Parameters, *Artificial Satellites, Journal of Planetary Geodesy*, Vol. **32**, No. 2, 75-85.
- Kosek W. and Kořaczek B., 1997. Semi-Chandler and Semiannual Oscillations of Polar Motion. *Geophysical Research Letters*, Vol. **24**, No 17, 2235-2238.
- Kosek W., McCarthy D.D., and Luzum B. 1998. Possible Improvement of Earth Orientation Forecast Using Autocovariance Prediction Procedures, *Journal of Geodesy* **72**, 189-199.
- Kosek W., 2000. Irregular short period variations in Earth rotation, *IERS Technical Note* **28**, 61-64.
- Kosek W. and Popiński W., 2000. Comparison between spectro-temporal analyses on the Earth Rotation Parameters and their excitation functions, *IERS Technical Note* **28**, 81-84.
- Kosek W., McCarthy D. D. and Luzum B. J., 2000. Prediction of complex-valued polar motion using the combination of autocovariance prediction and a least-squares extrapolation, paper presented at the EGS'2000 in Nice, France, 24-29 April, 2000.
- Kosek W., 2001. Autocovariance prediction of complex-valued polar motion time series, accepted to *Advances of Space Research*, February, 2001, paper presented at the 33rd COSPAR Scientific Assembly in Warsaw, 16-23 July, 2000.
- Lambeck K., 1980. *The Earth's variable rotation*, Cambridge University Press. New York.
- Lenhardt H. and Groten E., 1987. Chandler Wobble Parameters from BIH and ILS data, *Manuscripta Geodetica* **10**, 296-305.
- Malkin Z. and Skurikhina E., 1996. On Prediction of EOP, *Comm. IAA* **93**.
- Markowitz W., 1970. Sudden changes in rotational acceleration of the pole and secular motion of the pole, Mansinha L., Smylie D.E., and Beck A.E., (eds.) *Earthquake Displacement Fields and the Rotation of the Earth*, Reidel, Dordrecht, Netherlands, 69-81.

- McCarthy D.D. and Luzum B.J., 1991a, Combination of precise observations of the Orientation of the Earth, *Bulletin Geodesique*, **65**, 22.
- McCarthy D.D. and Luzum B.J., 1991b. Prediction of Earth Orientation, *Bull. Géod.*, **65**, 18-21.
- McCarthy D.D. and Luzum B.J., 1996. Path of the mean rotation pole from 1899 to 1994, *Geophys J. Int.* **125**, 623-629.
- Nastula J., Korsun A., Kołaczek B., Kosek W., and Hozakowski W., 1993. Variations of the Chandler and Annual Wobbles of Polar Motion in 1846-1988 and their Prediction, *Manuscripta Geodetica*, **18**, 131-135.
- NOAA 2001. Climate Prediction Center – Data: Current Monthly Atmospheric and SST index values, <http://www.cpc.ncep.noaa.gov/data/indices/>
- Okubo S., 1982. Is the Chandler period variable ?, *Geophys. J. R. Astr. Soc.* **71**, 629-646.
- Popiński W. and Kosek W. 1995. The Fourier Transform Band Pass Filter and its Application to Polar Motion Analysis, *Artificial Satellites*, Vol. **30**, No 1, 9-25.
- Priestley M.B. 1981. *Spectral Analysis and Time Series*, Academic Press, London.
- Rovelli A., and Vulpiani A., 1983. Characteristic Correlation Time as Estimate of Optimum Filter Length in Maximum Entropy Spectral Analysis, *Geophys. J. R. Astr. Soc.* **73**, 293-306.
- Schuh H. and Schmitz-Hübsch H., 2000. Short period variations in Earth rotation as seen by VLBI, *Surveys in Geophysics* **21**, 499-520.
- Schuh H., Nagel S., and Seitz T., 2001a. Linear drift and periodic variations in long time series of polar motion, *Journal of Geodesy*, **74**, 701-710.
- Schuh H., Ulrich M., Egger D., Müller J. and Schwegmann W., 2001b. Prediction of Earth orientation parameters by neural networks, submitted to *Journal of Geodesy*.
- USNO, 2001. finals.all: all NEOS EOP values since 12 Jan 1973 (with 1 year of predictions) <http://maia.usno.navy.mil/>
- Vicente, R.O. and Wilson C.R., 1997. On the variability of the Chandler frequency, *Journ. Geophys. Res.*, Vol. **102**, No B9, 20439-20445.
- Vondrak J., 1985. Long period behavior of polar motion between 1900 and 1984, *Ann. Geophys.*, **3**, 351-356.
- Vondrak J., 1989. Prediction of Polar Motion from the Air and Water Excitation, Report No 402, Department of Geodetic Science and Surveying, The Ohio State University, Columbus, Dec, 1989.
- Vondrak J., 1999a. Earth Rotation Parameters 1899.7 – 1992.0 after reanalysis within the HIPPARCOS frame, *Surv. Geophys.* **20**, 169-195.
- Vondrak J., 1999b, Secular and long periodic polar motion as derived from combination of astrometric and space geodetic observations, In: Capitaine N. (ed) *Journées 1998, Systèmes de Référence Spatio-Temporels*, Paris, Sep. 1998, Observatoire de Paris, UMR 8630/CNRS, 195-201.

Yatskiv Ya. S., Korsun A.A., Rykhlova L.V., 1972, On the spectrum of polar coordinates from 1884 to 1971, *Russian Astron. Journal*, Vol. **49**, 6, 1311-1318.

Zhu S. Y. 1981. Prediction of Earth rotation and polar motion, Reports of the Department of Geodetic Science and Surveying, *Report No. 320*, Columbus, Ohio.

Zhu S. Y. 1982. Prediction of polar motion, *Bull. Géod.* **56**, 258-273.